

# Application of a physiologically based pharmacokinetic/pharmacodynamic (PBPK/PD) model for prediction of drug-drug interactions (DDIs) involving the JAK1/2 inhibitor Ruxolitinib in Caucasians and Japanese

## Background

Ruxolitinib is metabolized by CYP3A4, CYP2C9 and CYP1A2 and reported fm values are 0.79, 0.16 and 0.05 [1], respectively. However, a DDI with ketoconazole (200mg BID, 3 days) led only to a 2-fold change in AUC [2], indicating that the *in vivo* fm for CYP3A4 is closer to 0.5 than 0.79.

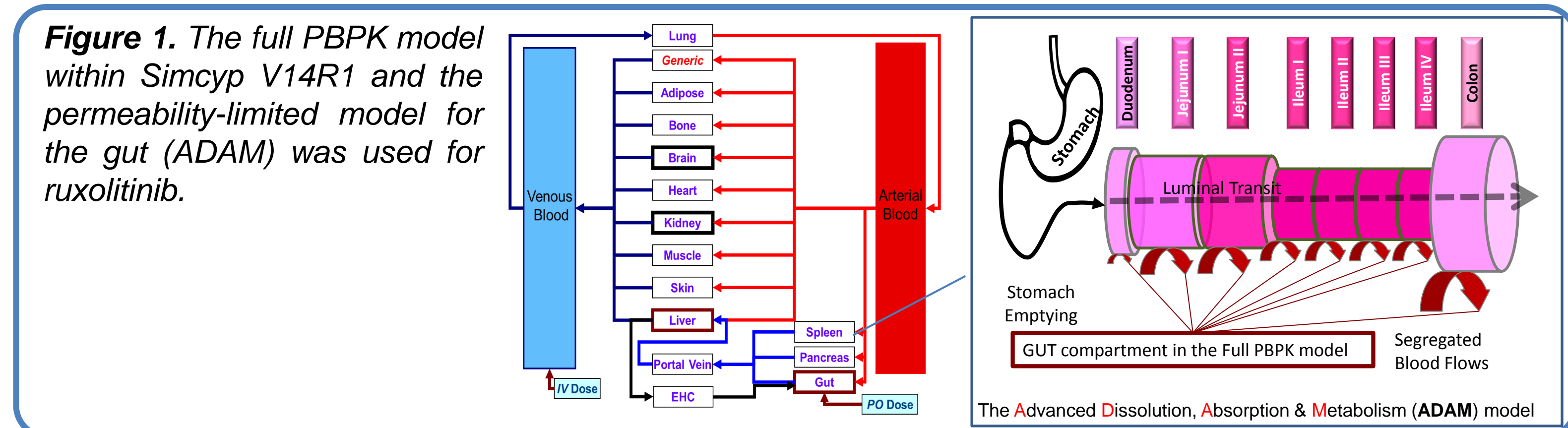
## Objectives

To develop PBPK/PD models to assess the drug interactions between ruxolitinib (substrate of CYP2C9, CYP3A4, CYP1A2; inhibitor of P-gp) and ketoconazole (CYP3A4 inhibitor), erythromycin (CYP3A4 and CYP2C9 inhibitor), rifampicin (CYP1A2, CYP2C9 and CYP3A4 inducer) or digoxin (P-gp substrate) in healthy Caucasian and Japanese volunteers.

## Methods

### Ruxolitinib PBPK model

Available *in vitro* and *in vivo* information on the metabolism of ruxolitinib was combined with physicochemical data within the Simcyp Population-based Simulator (V14R1). A whole body PBPK model was constructed, where the Advanced Dissolution, Absorption and Metabolism (ADAM) model was utilised to describe the absorption for the compound (**Figure 1**). Permeability was estimated from physicochemical and Caco-2 cell data using the Mech P<sub>eff</sub> model, while the intrinsic solubility was calculated using SIVA (V1.0), including an intestinal uptake transporter, to recover the early C<sub>max</sub>.



In addition to renal filtration, intestinal (CYP2C9 and CYP3A4) and hepatic metabolism (CYP2C9, CYP3A4 and CYP1A2), an additional clearance was included in the model to recover the observed oral clearance and AUC ratios reported in the Ketoconazole DDI study [2]. Reported *in vivo* CL<sub>po</sub> and CL<sub>R</sub> were used to back-calculate a metabolic intrinsic clearance using a retrograde approach. The fm values of 0.53 for CYP3A4, 0.12 for CYP2C9, 0.03 for CYP1A2, 0.014 as renal and 0.29 as additional clearance were used.

To test the Ruxolitinib PBPK model, the default healthy volunteer Caucasian and Japanese physiology models were used. A population file for African-American subjects was created accounting for known ethnic differences in CYP expression. Simulations were run to generate plasma concentrations of ruxolitinib following single doses (SD) and multiple doses (MD) in healthy volunteers.

### DDI studies

The default PBPK models in Simcyp for the CYP inhibitors, ketoconazole and erythromycin, and the P-gp substrate, digoxin, were used without modification. Rifampicin induction effects on CYP1A2 and CYP2C9 were simulated by increasing enzyme abundance data of 1.2 and 1.4-fold, respectively, and induction by CYP3A4 was addressed using the default semi-mechanistic induction model [3]. The simulated plasma concentrations of ruxolitinib were consistent with observed data across 8 independent test studies, including 3 DDI studies at inhibitor dose of 200 mg BID ketoconazole (3 days); 500 mg BID erythromycin (3 days) and 600 mg QD rifampicin (10 days) in Caucasian subjects.

### Pharmacodynamics

The pharmacodynamic effects of ruxolitinib (10-50 mg), as judged by changes in STAT3 phosphorylation state, were included in the model using a sigmoid E<sub>max</sub> model with a delay compartment.

## Results

● The simulated plasma concentrations of ruxolitinib were consistent with observed data in 8 test studies in Caucasian/Black and 6 external test studies in Japanese healthy volunteers (Examples are shown in **Figures 2A-D**).

● The robustness of the PBPK model was demonstrated by its ability to recover the observed AUC and C<sub>max</sub> within 1.6-fold across 25 clinical studies, including six MD studies in Japanese subjects (**Figures 3A and B**).

● Simulated change in the pharmacokinetic profile of ruxolitinib due to the co-medication of ketoconazole (**Table 1**; trainings set), erythromycin (**Table 1, Figure 4**, test set) or rifampicin (**Table 1, Figure 5**; test set) were in line with observed data.

● The pharmacodynamics of ruxolitinib given alone were reasonable well described (**Figure 6**) but the pharmacodynamic effects after co-medication that affected the CYP3A4 metabolic pathways were under predicted as the model did not account for the effects of an active ruxolitinib metabolite.

### PK profiles of Ruxolitinib in Healthy Volunteers

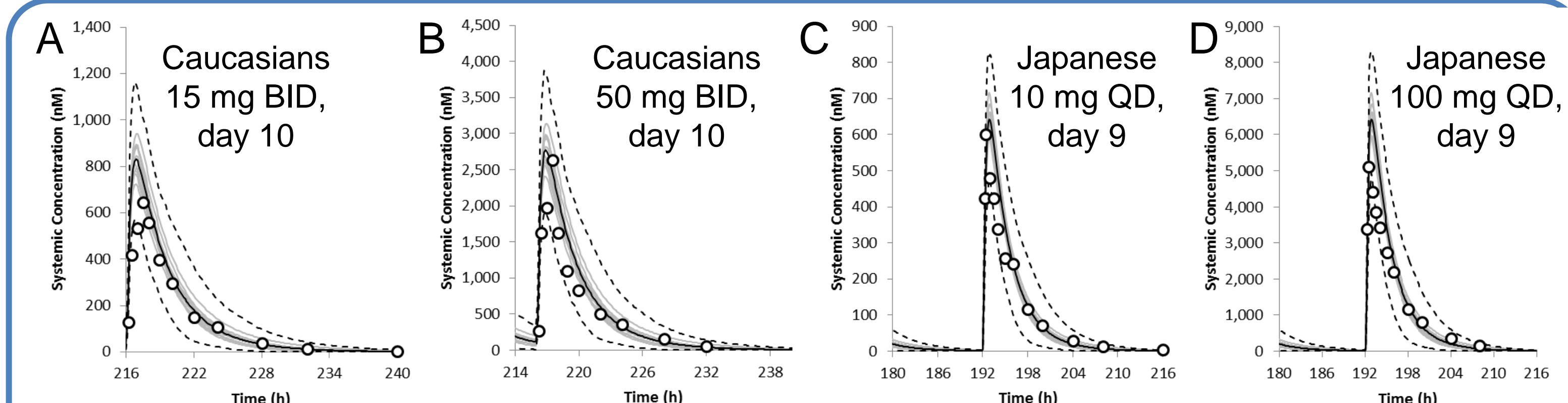


**Figure 2.** Simulated (black line) and observed (data points) mean plasma concentration profiles of ruxolitinib after multiple oral doses to (A, B) healthy Caucasians and (C, D) Japanese. The grey lines represent predictions from 10 individual trials; dashed lines are 5<sup>th</sup> and 95<sup>th</sup> percentile.

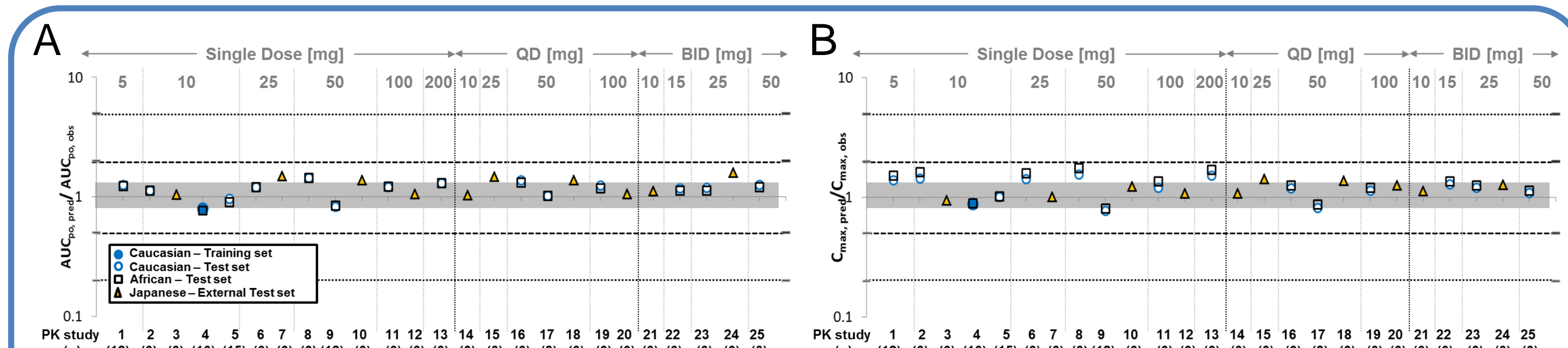


**Figure 3.** (A) AUC ratios (predicted/observed) and (B) C<sub>max</sub> ratios (predicted/observed) of 25 clinical studies reported in the literature [2, 4, 5]. Key: (●) Trainings set; (○) Test set in Caucasians; (□) Test set in African-Americans; (Δ) external test set in Japanese.

### CYP3A4, CYP2C9 and CYP1A2-mediated DDIs

The predicted increase in exposure of ruxolitinib following co-administration of CYP inducers and inhibitors was consistent with observed data (**Table 1**), prospectively a DDI with Digoxin was estimated as negligible.

**Table 1** Predicted and observed ruxolitinib drug interactions

Inhibitor	Observed geometric mean	Simulated geometric mean
	AUC <sub>R</sub> (90% CI)	AUC <sub>R</sub> (range in individual trials)
Ketoconazole*	1.91 (1.72 – 2.12)	2.06 (1.88 – 2.29)
Erythromycin*	1.27 (1.17 – 1.38)	1.47 (1.41 – 1.52)
Rifampicin**	0.29 (0.21 – 0.40)	0.37 (0.32 – 0.40)
Digoxin**,# (0.5 mg SD)	prospective	1.00 (1.00-1.01)

\*10mg SD RUX; \*\*50mg SD RUX; fu<sub>gut</sub>=fu\*CL<sub>50,P-gp</sub>/2 = K<sub>i</sub> = 10.75 μM

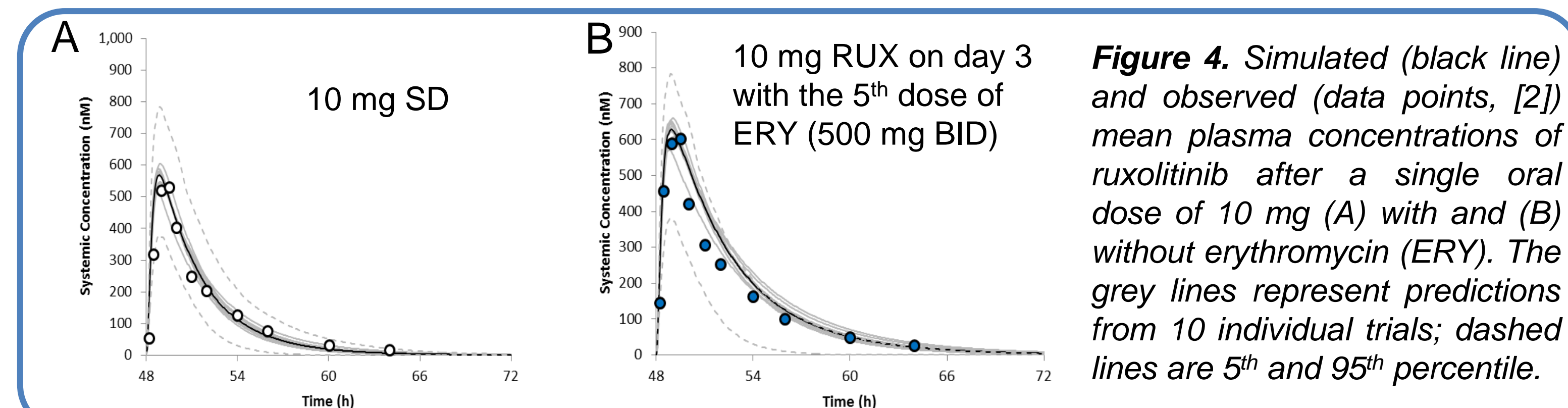


**Figure 4.** Simulated (black line) and observed (data points, [2]) mean plasma concentrations of ruxolitinib after a single oral dose of 10 mg (A) with and (B) without erythromycin (ERY). The grey lines represent predictions from 10 individual trials; dashed lines are 5<sup>th</sup> and 95<sup>th</sup> percentile.

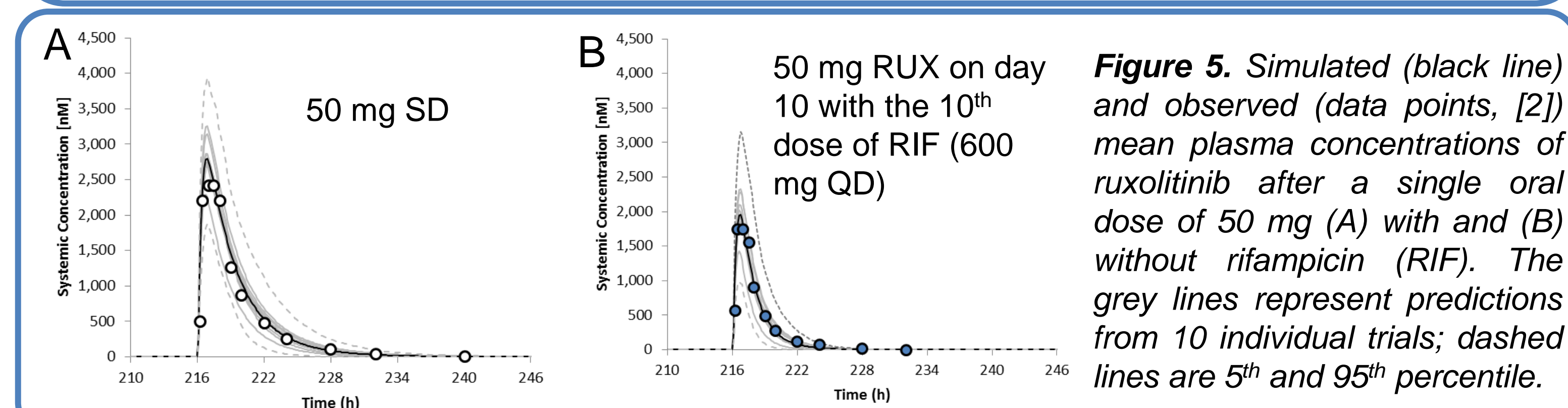


**Figure 5.** Simulated (black line) and observed (data points, [2]) mean plasma concentrations of ruxolitinib after a single oral dose of 50 mg (A) with and (B) without rifampicin (RIF). The grey lines represent predictions from 10 individual trials; dashed lines are 5<sup>th</sup> and 95<sup>th</sup> percentile.

### Pharmacodynamics

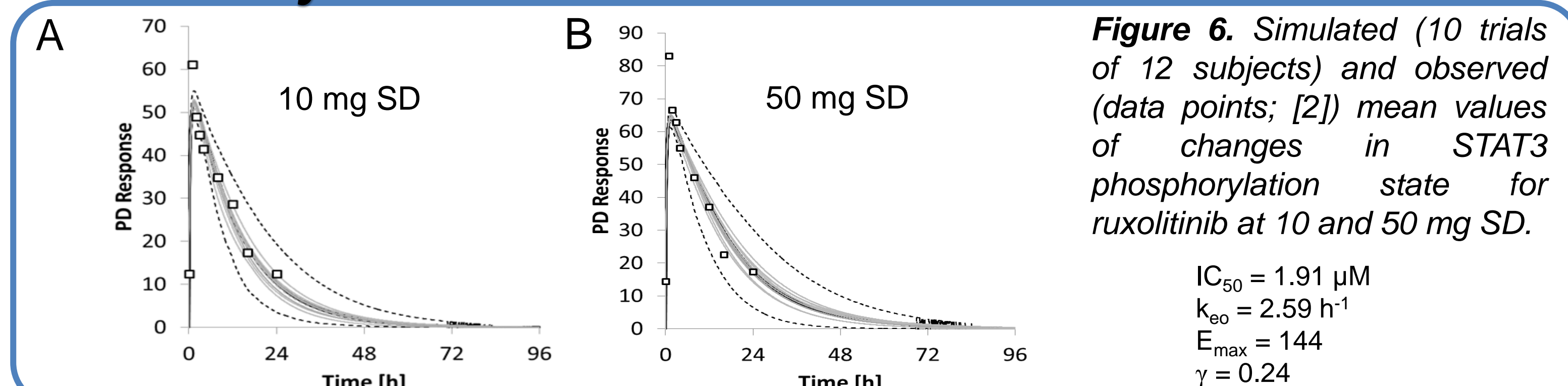


**Figure 6.** Simulated (10 trials of 12 subjects) and observed (data points; [2]) mean values of changes in STAT3 phosphorylation state for ruxolitinib at 10 and 50 mg SD.

## Conclusions

- A **single** PBPK model for ruxolitinib was able to recover PK profiles over a wide range of doses in Caucasians, African-American and Japanese subjects when population specific physiological differences were accounted for.
- PBPK modelling in conjunction with reliable *in vitro* data can be used to assess the importance of interactions affecting metabolism via CYP2C9, CYP3A4 and CYP1A2 for ruxolitinib.
- Prospective predictions based upon the **same** verified PBPK model for digoxin are presented.
- The plasma concentration generated with the **same** PBPK model were used as input for a PD model capable to describe effects, when ruxolitinib was given alone.

**Outlook:** To account for the effect of the active CYP3A4 metabolite, the model needs to be extended to simulated kinetics of that metabolite. Also PD feedback leading to changes in small intestinal transit time (e.g., ERY) could be further evaluated with this PBPK model of ruxolitinib.

### References

- [1] Shi *et al.*, 2015 CPT 97(2):177-185.
- [2] Shi *et al.*, 2012 JCP 52:809-818.
- [3] Almond *et al.*, 2009 Curr Drug Metab 10(4):420-432.
- [4] Shi *et al.*, 2011 JCP 51:1644-1654.
- [5] Ogama *et al.*, 2013 Int J Hematol 97:351-359.